doi: 10.18323/2782-4039-2024-3-69-2

Corrosion-mechanical destruction of bainite structures in oilfield environments

Mikhail A. Vyboishchik[1,3], Doctor of Sciences (Physics and Mathematics), Professor,
professor of Chair "Welding, Pressure Treatment of Materials and Allied Processes"
Igor V. Gruzkov*[1,2,4], postgraduate student,
Head of the Laboratory of Optical and Electron Microscopy
[1]*Togliatti State University, Togliatti (Russia)*
[2]*IT-Service Limited Liability Company, Samara (Russia)*

***E-mail:** gruzkov@its-samara.com,
gigabon7@mail.ru

[3]ORCID: https://orcid.org/0000-0003-2797-5396
[4]ORCID: https://orcid.org/0009-0007-9580-9935

Received 12.12.2023 *Accepted 15.08.2024*

Abstract: The main direction in solving the problem of increasing the reliability of field equipment, is the creation of new steels with higher resistance to corrosion-mechanical destruction. Currently, to produce oil and gas pipeline systems, low-carbon, low-alloy steels are used, in which lath carbide-free bainite is formed when quenched in water. Such a structure provides a combination of high strength and resistance to brittle fracture. However, issues of increasing corrosion resistance are still open. The purpose of this work is to identify the structural condition of low-carbon, low-alloy, pipe steels, providing a combination of high mechanical properties with increased corrosion resistance in oilfield environments. The studies were carried out on the latest generation 08KhFA, 08KhFMA and 05KhGB steels, most popular when manufacturing oil and gas pipelines. Samples for the study were cut from the pipes and quenched from the austenite region in water, which formed the structure of lath carbide-free bainite. The quenched samples were tempered at temperatures of 200, 300, 400, 500, 600, and 700 °C. To identify the relationship between the morphology of bainite structures and their properties, the samples after quenching and tempering at each temperature, were subjected to metallographic analysis, X-ray diffraction analysis, mechanical tests, and corrosion resistance tests. The work shows the sequence of structure transformation, temperature ranges of phase and structural transformations, changes in mechanical properties, and corrosion resistance that occur during tempering of lath carbide-free low-carbon bainite. It is shown that tempering of lath carbide-free bainite (08KhFA, 08KhMFA and 05KhGB steels) does not affect the rate of carbon dioxide corrosion. It has been found that medium tempering forms the structural condition of carbide-free low-carbon lath bainite providing a combination of high mechanical properties and high corrosion resistance in oil field environments. For each of the steels under study, the authors give recommended heat treatment modes.

Keywords: corrosion-mechanical destruction; destruction of bainite structures; oilfield environment; pipe steels; structural condition.

For citation: Vyboishchik M.A., Gruzkov I.V. Corrosion-mechanical destruction of bainite structures in oilfield environments. *Frontier Materials & Technologies*, 2024, no. 3, pp. 17–29. DOI: 10.18323/2782-4039-2024-3-69-2.

INTRODUCTION

The constant increase in the aggressiveness of oilfield environments, and the intensity of oil production (injection of water and carbon dioxide into the formation) [1], leads to a sharp increase in the rate of corrosion-mechanical destruction of oilfield equipment. A significant improvement of the mechanical properties and corrosion resistance of the pipe steels used is required. High alloying, significantly increases the cost of steel, and in some cases, reduces the strength properties. Other approaches ensuring high resistance to corrosion-mechanical destruction are required. Currently, low-carbon low-alloy steels with a bainite structure after quenching in water are used for the production of oil and gas pipeline systems (pipes and pipeline fittings). Bainite structures having a unique combination of high strength and ductility provide high resistance to mechanical destruction of pipe steels [2–4]. The formation of the bainite structure, and the relationship of their structural condition with mechanical properties are described in sufficient detail [5–7]. The most complete classification of bainite structures is given in [8]. Bainite structures of low-carbon low-alloy steels are singled out as a separate group and considered in works [5; 9]. The preferred structure providing the highest plastic properties of these steels is lath carbide-free bainite, in which residual (untransformed) austenite is located at the boundaries of the laths, that causes high resistance to brittle fracture [6; 10; 11].

At the same time, it should be noted that, despite a large number of studies of bainitic steels, the issues of changes in the structure and properties of bainite structures, with an increase in tempering temperature, have not been sufficiently studied, and the relationship between the morphology of bainites and their corrosion resistance has barely been considered. Such information is necessary for a practical solution to the issue of increasing the reliability of pipe steels.

The purpose of this work is to find the structural condition of low-carbon low-alloy pipe steels, providing a combination of high mechanical properties with increased corrosion resistance in oilfield environments.

METHODS

08KhFA, 08KhMFA and 05KhGB steels were selected for the study. Their elemental composition (Table 1) and thermokinetic diagrams of the supercooled austenite decomposition (Fig. 1) are given according to the data of the manufacturer. In 08KhMFA steel, compared to 08KhFA steel, the carbon content is reduced from 0.09 to 0.05 % and 0.2 % of Mo is introduced. 05KhGB steel is additionally alloyed with niobium, and due to the favorable Mn/Si ratio, has higher weldability.

All samples were water-quenched (20 °C) from the austenitic region (08KhFA and 08KhMFA steels – from a temperature of 930 °C, 05KhGB steel – from 920 °C), and then tempered at 200, 300, 400, 500, 600, and 700 °C.

Table 1. *Chemical composition of steels under study*
Таблица 1. *Химический состав исследуемых сталей*

Steel grade	Weight fraction of elements, %											
	C	Si	Mn	Cr	Ni	Cu	Nb	V	Mo	Al	S	P
08KhFA	0.09	0.20	0.44	0.52	0.12	0.11	0.020	0.088	0.003	0.034	0.002	0.011
08KhMFA	0.05	0.39	0.39	0.70	0.10	0.17	0.011	0.061	0.190	0.057	0.004	0.003
05KhGB	0.05	0.22	0.71	0.61	0.08	0.18	0.029	0.003	0.010	0.013	0.001	0.006

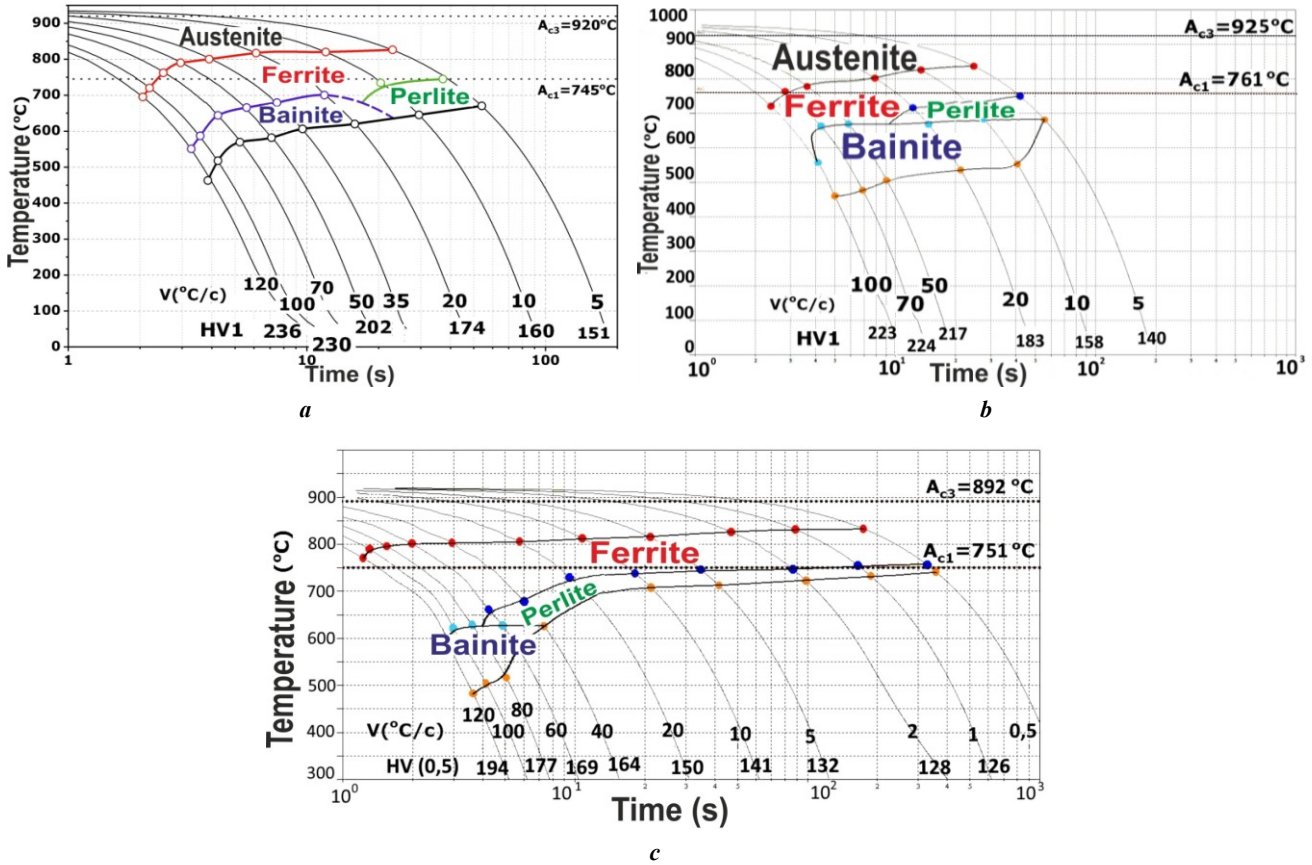

Fig. 1. *Thermokinetic diagrams of decomposition of supercooled austenite of steels under study:*
a *– 08KhFA steel;* ***b*** *– 08KhMFA steel;* ***c*** *– 05KhGB steel.*
The diagrams are based on the data from Vycsa metallurgical plant
Рис. 1. *Термокинетические диаграммы распада переохлажденного аустенита исследуемых сталей:*
а *– сталь 08ХФА;* ***b*** *– сталь 08ХМФА;* ***c*** *– сталь 05ХГБ.*
Диаграммы приведены по данным Выксунского металлургического завода

Quenching from the austenitic region provides a large amount of bainite component in the steel structure, and water is the most technologically advanced medium. For each tempering temperature, the structural condition was studied and mechanical and corrosion properties due to this structure were determined.

To conduct the studies, longitudinal strips measuring 120×20×7 mm were cut from Ø146×7 mm pipes produced using conventional factory technology. The strips were subjected to heat treatment, and then samples were made from them. To ensure identical and relatively homogeneous structural condition, all samples were subjected to normalisation (08KhFA and 08KhMFA steels at a temperature of 940 °C, 05KhGB steel at 930 °C, holding time – 30 min), with cooling in still air. This ensured similar grain sizes and identical ferrite-pearlite structure, with lamellar cementite in pearlite in the samples before heat treatment.

The research and testing methods are presented in the form of groups according to their purpose.

Metallographic analysis included light microscopy (GX51 microscope, Olympus, Japan), SEM electron scanning microscopy (XL-30 microscope, Philips, Netherlands), EBSD technique (identifying intergranular disorientation angles), TEM transmission electron microscopy (EMV-100L microscope, Russia), and diffraction analysis.

Quantitative assessment of structural components was carried out using Thixomet Pro software.

X-ray diffraction analysis for volumetric determination of phase composition and stress state (3^{rd} type residual stresses and dislocation density), was performed using a Shimadzu Maxima XRD-7000S diffractometer, Japan (Cu-Kα radiation, tube power is 1.6 kW) in the angle range of 40–100°. Crystalline phases were identified using the Shimadzu PDF2 database. Full-profile analysis of diffraction patterns was performed using the LeBel and Rietveld methods in the Jana2006 program.

Hardness tests (GOST 9013), uniaxial tensile tests (GOST 1497), and impact toughness tests (GOST 9454) were performed to determine mechanical properties.

To determine resistance to corrosion destruction, hydrogen cracking tests (NACE TM0284 standard), sulfide stress corrosion cracking tests (NACE TM0177 standard), carbon dioxide corrosion resistance tests (technique developed by IT-Service LLC, 400-hour exposure in an aggressive environment with 3.5 % of chlorides at 65 °C, and a CO_2 pressure of 0.1 MPa, which allowed creating corrosion products on the sample surface similar to those that form in real conditions during many months of operation in carbon dioxide oilfield environments), were carried out.

RESULTS

Phase transformations during cooling

Thermokinetic diagrams of austenite decomposition in 08KhFA, 08KhMFA and 05KhGB steels (Fig. 1), and panoramic images of changes in the structure of these steels along the length of the sample during end quenching (Fig. 2), provide an idea of the effect of the cooling rate on the formation of the structure of steels. The studied steels acquire a bainite structure after water quenching. 08KhMFA steel has a wider range of cooling rates that form bainite structures (Fig. 1). Continuous hardenability for all steels is ensured to a depth of 10 mm.

The studied steels have one type of bainite structure and a similar nature of its change upon heating therefore, the ongoing processes of structure transformation and property changes (Fig. 3–5), are shown using the example of one steel – 08KhMFA steel with higher corrosion resistance.

Structural condition after quenching

After water quenching, a structure consisting of lath carbide-free bainite with thin layers of residual austenite, and a small proportion of excess ferrite localised along the boundaries of the former austenite grain, is formed in the steels under study (Fig. 3).

The amount of excess ferrite is insignificant – from 3 to 10 %, the largest amount is in 05KhGB steel. Ferrite is located mainly along the boundaries of the former austenite grain. Bainite consists of laths of bainitic ferrite, along the boundaries of which there are thin layers of residual austenite. Ordered sequence of bainite laths and layers of residual austenite predominates. The width of the laths for the steels under study varies from 200 to 800 nm.

Wider laths (average width is ≈600 nm), are observed in sections of 08KhMFA steel. The amount of residual austenite is 0.5–1.5 %. X-ray diffraction analysis reveals only its traces. Microdiffraction analysis of transmission electron microscopy images identified the γ-phase (Fig. 3 c). With a small amount, residual austenite in the form of thin layers (≈40 nm) located along the boundaries of bainitic ferrite laths determines the mechanical properties (high ductility) of carbide-free bainites in low-carbon steels.

Thus, 08KhFA, 08KhMFA, 05KhGB steels after quenching, have a structure of lath carbide-free bainite with close parameters of the structural condition.

The evolution of the structural condition with an increase in the tempering temperature is shown in Fig. 4, 5. During tempering, as the temperature increases to Ac_1, a successive transition of carbide-free lath bainite, with excess ferrite along the grain boundaries into a mixture of ferrite with globular carbide particles occurs (Fig. 4, 5). The fine grain obtained during quenching (numbers 9–11 according to GOST 5639) in the tempering temperature range of up to 700 °C remains virtually unchanged. A further increase in the tempering temperature (730 °C) for 08KhFA steel leads to the development of secondary recrystallisation processes and a sharp grain growth. With an increase in the tempering temperature, a constant increase in the intergranular disorientation angles, and accordingly, an increase in the proportion of high-angle boundaries is observed in the studied steels, which causes an increase in plasticity. It is characteristic that the high dislocation density after quenching $(3–5)\times10^{14}$ m^{-2} remains virtually unchanged, up to a tempering temperature of 600 °C (Table 2). The 3^{rd} type residual stresses decrease continuously with increasing tempering temperature, especially intensively from 400 °C (Table 2).

The results of mechanical tests, impact bending tests, as well as the assessment of the 3^{rd} type residual stresses and dislocation density are given in Table 2.

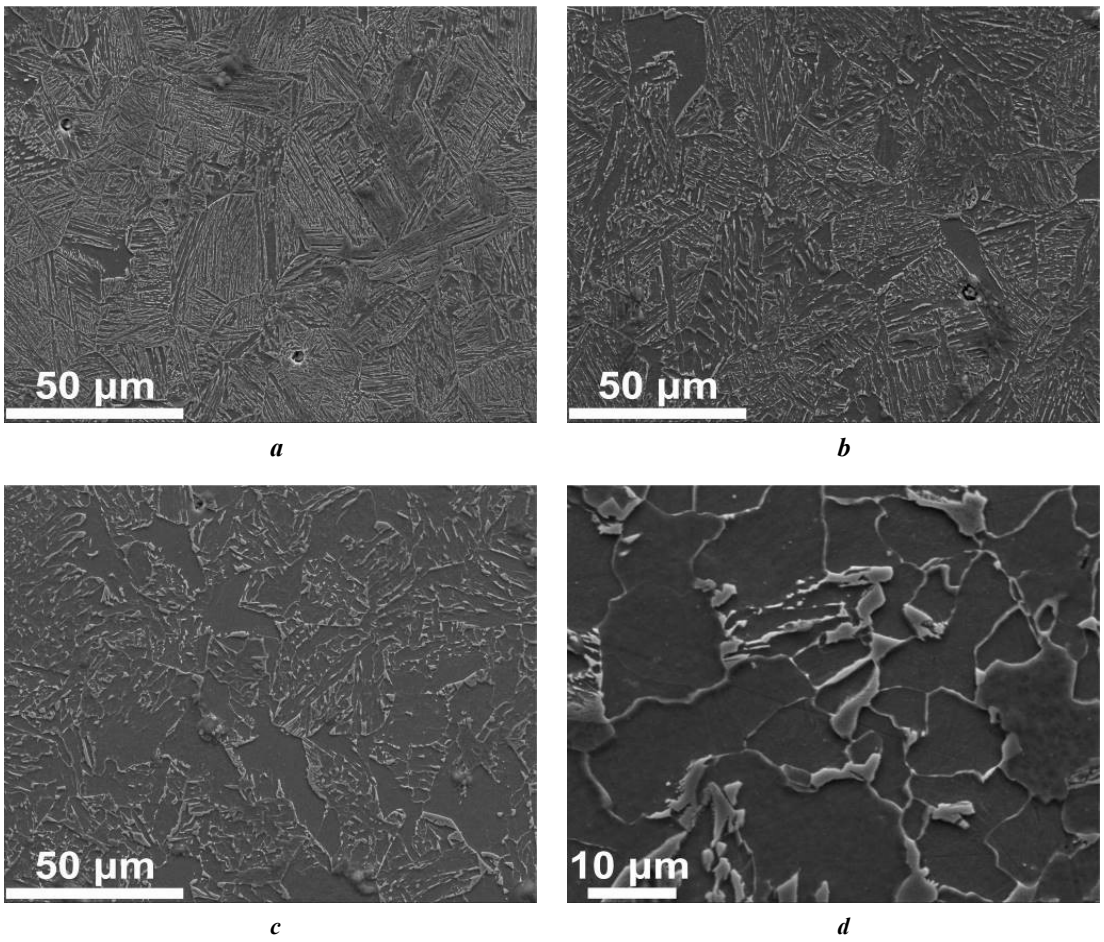

Fig. 2. *Change in the structure of 08KhMFA steel during end quenching:* ***a*** *– distance from the sample end is h=2 mm, hardness is 298 HV;* ***b*** *– h=7 mm, 235 HV;* ***c*** *– h=12 mm, 205 HV;* ***d*** *– h=17 mm, 176 HV*

Рис. 2. *Изменение структуры стали 08ХМФА при торцевой закалке:* ***a*** *– расстояние от торца образца h=2 мм, твердость 298 HV;* ***b*** *– h=7 мм, 235 HV;* ***c*** *– h=12 мм, 205 HV;* ***d*** *– h=17 мм, 176 HV*

The change in resistance to corrosion destruction in oilfield environments with increasing tempering temperature is given in Table 3 and shown in Fig. 6, 7.

DISCUSSION

Changes in structure and properties with increasing tempering temperature

Structure

After tempering at 200 °C, the residual austenite disappears. This is also observed in 08KhFA [12] and 05KhGB [13] steels. The temperature stability of the residual austenite or complex (austenite-martensite phase) is considered in [14; 15], the effect of V and Nb microadditives is considered in [16; 17], where it is indicated that with a particle size of 0.5–3 μm, the austenite decomposition occurs in the temperature range of 300–400 °C [14; 15]. In the lath bainite of the steels under study, untransformed austenite is in the form of thin layers (≈40 nm), and its decomposition can be expected at lower temperatures. Estimated calculations show that after 30 min of holding at a temperature of 200 °C, the distance of diffusion of carbon atoms from austenite is more than an order of magnitude greater than the width of the interlayers and fully ensures the residual austenite decomposition [12]. The type of austenite transformation (martensite, bainite or α-ferrite) remains debatable.

Further transformation of the structure is associated with the formation and growth of carbides, the development of polygonisation and recrystallisation processes. The change in the structural condition of lath carbide-free bainite, with an increase in the tempering temperature occurs in the following sequence:

– at 200 °C, untransformed austenite disappears;

– when tempering at 300 °C, the first needle-shaped iron carbide precipitates appear;

– in the temperature range of 400–500 °C, carbide particles appear throughout at the boundaries of the laths, they coalesce and spheroidise, and chains of carbide inclusions appear at the boundaries of bainitic laths (Fig. 5 b and 5 c). 3rd type residual stresses decrease sharply (Table 2), which indicates the transition of carbon from the crystal lattice to a bound state in the form of carbides. Polygonisation processes develop: a decrease in low-angle boundaries and an increase in high-angle ones, while the dislocation density remains virtually unchanged;

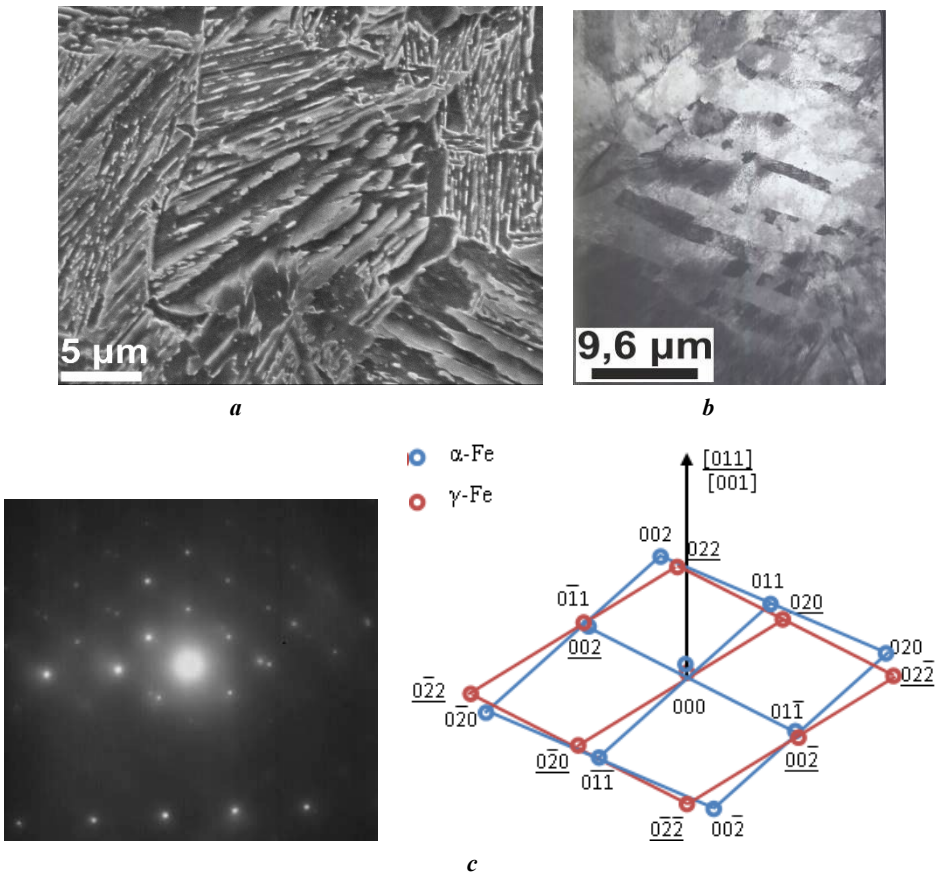

a *b* *c*

Fig. 3. *Microstructure of 08KhMFA steel after quenching:* ***a*** *– SEM;* ***b*** *– TEM (bright-field image);* ***c*** *– microdiffraction*
Рис. 3. *Микроструктура стали 08ХМФА после закалки:*
a *– СЭМ;* ***b*** *– ПЭМ (светлопольное изображение);* ***c*** *– микродифракция*

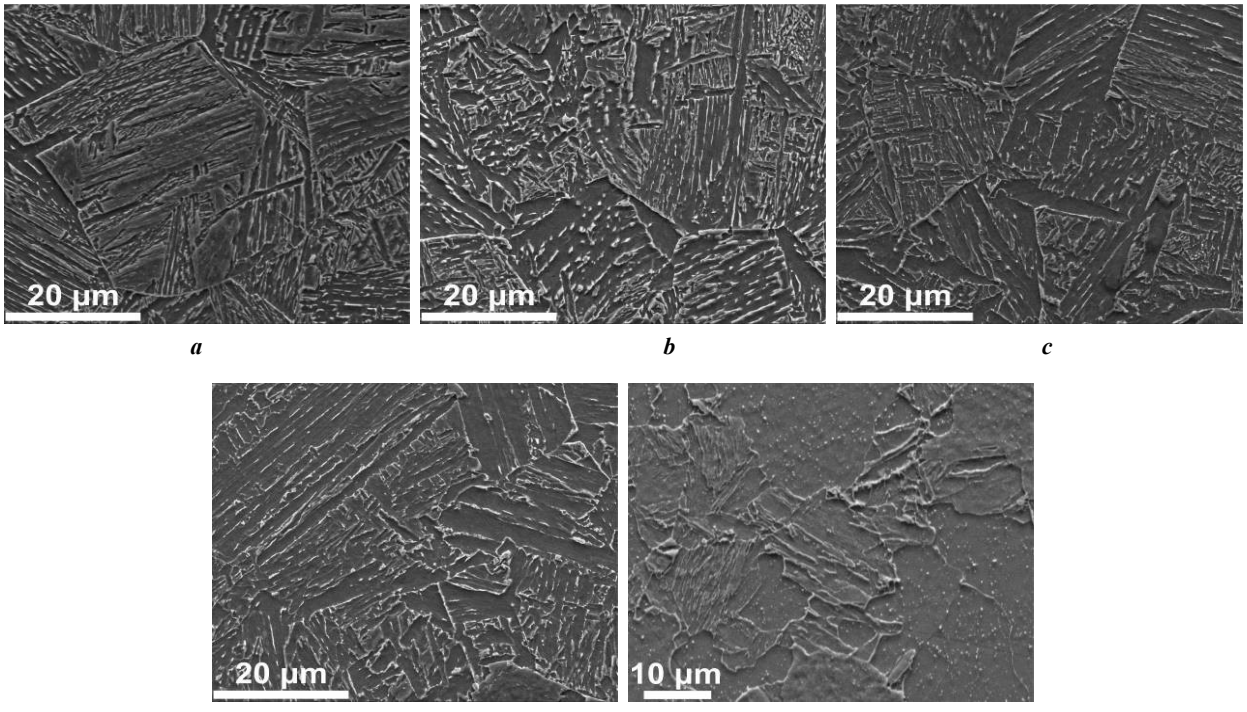

a *b* *c*

d *e*

Fig. 4. *Structure of 08KhMFA steel after quenching from the temperature of 930 °C and tempering at:*
a *– 200 °C;* ***b*** *– 300 °C;* ***c*** *– 400 °C;* ***d*** *– 500 °C;* ***e*** *– 700 °C. SEM*
Рис. 4. *Структура стали 08ХМФА после закалки с температуры 930 °С и отпуска при:*
a *– 200 °C;* ***b*** *– 300 °C;* ***c*** *– 400 °C;* ***d*** *– 500 °C;* ***e*** *– 700 °C. СЭМ*

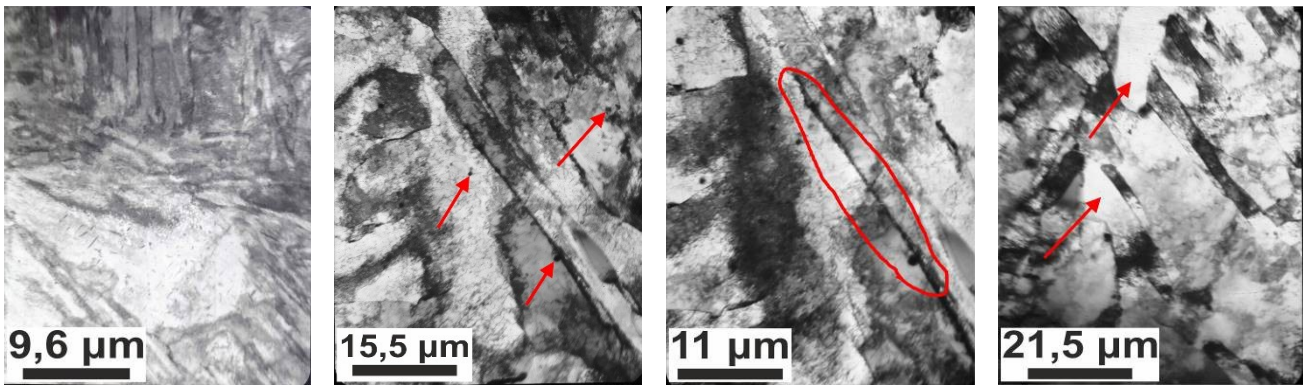

Fig. 5. *Change in the structure of 08KhMFA steel with the growth in the tempering temperature (TEM):*
a *– tempering at 300 °C;* ***b*** *– tempering at 400 °C (arrows indicate globular carbides);*
c *– tempering at 500 °C (carbide chains are encircled);* ***d*** *– tempering at 600 °C (arrows indicate recrystallisation nuclei)*
Рис. 5. *Изменение структуры стали 08ХМФА с ростом температуры отпуска (ПЭМ):*
a *– отпуск при 300 °С;* ***b*** *– отпуск при 400 °С (стрелками показаны глобулярные карбиды);*
c *– отпуск при 500 °С (обведены цепочки карбидов);* ***d*** *– отпуск при 600 °С (стрелками показаны зародыши рекристаллизации)*

– from a tempering temperature of 600 °C (Fig. 5 d), the main factor determining the change in structure and properties is the intensity of recrystallisation processes. Carbide reactions of cementite replacement by special carbides are possible;

– tempering at a temperature above 700 °C can cause secondary recrystallisation and a sharp grain growth (08KhFA steel).

Mechanical properties

Usually, in pipe production technologies, bainite structures are subjected to high tempering by analogy with martensite structures. For pipes made of low-carbon low-alloy steels, this is 600–750 °C, when partial recrystallisation significantly reduces strength [18]. There is some information on the effect of lower tempering temperatures on the properties and morphology of bainite [19; 20], but no general picture of changes in mechanical properties during tempering has been found in the literature.

The authors studied changes in the structure, mechanical properties, and corrosion resistance over the entire tempering temperature range (20–730 °C), which is 50 °C below the Ac_1 line, for 08KhFA, 08KhMFA, and 05KhGB steels.

An increase in temperature to 730 °C for 08KhFA steel led to a sharp increase in grain size. The steels under study after quenching and subsequent tempering to a temperature of 600 °C are characterised by a combination of high strength and plastic properties (Table 2), which for most heat treatment modes is higher than the requirements of K52 strength group. Characterising the thermal stability of mechanical properties, one can note that the strength properties (σ_{UTS} and $\sigma_{0.2}$) remain virtually unchanged upon tempering to a temperature of 400 °C. Apparently, this is associated with the appearance of precipitates of dispersed cementite particles. The plasticity characteristics (δ and KCV-50) after quenching are quite high and increase with a growth of the tempering temperature (Table 2). A sharp softening appears from a tempering temperature of 600 °C, which is caused by an increase in the intensity of recrystallisation processes. On the whole, the general nature of the change in mechanical properties for the three steels under study is identical.

Corrosion resistance

Steels in aggressive oilfield environments are subjected to the following types of corrosion destruction: hydrogen cracking (HC), sulfide stress corrosion cracking (SSCC), carbon dioxide and bacterial corrosion [21; 22]. The studied low-carbon chromium-containing steels (≈0.6 % of Cr) are relatively resistant to biocorrosion [22]. Modification with rare earth metals (REM) significantly increases their resistance to bacterial attack. The main problem is to ensure resistance to carbon dioxide corrosion.

The obtained values of HC, SSCC and carbon dioxide corrosion rate (Table 3) indicate, that the studied steels have increased corrosion resistance in oilfield environments, compared to traditionally used 20, 20F, 17G1, 09G2S pipe steels.

An interesting and unexpected result is that tempering of low-carbon steels with a lath carbide-free bainite structure, has virtually no effect on the intensity of carbon dioxide corrosion. With an increase in tempering temperature to 700 °C, the structural condition changes from lath carbide-free bainite to a ferrite-carbide mixture and the carbon dioxide corrosion rate remains constant. This phenomenon is characteristic of all the steels under study (Table 3, Fig. 6). The correctness of the obtained corrosion rate values is also confirmed by the proximity and similarity of the curves for changing the Fe^{+2} concentration in the corrosion environment during testing (Fig. 7). These curves also characterise the kinetics of corrosion processes, and the influence of corrosion products on the intensity of corrosion destruction. For the steels under study, the nature of the change in the corrosion rate depending on the test time is similar (Fig. 6).

According to existing concepts, the rate of carbon dioxide corrosion of steels is determined by the formation

Table 2. *Dependence of mechanical properties, residual stresses and dislocation density of 08KhFA, 08KhMFA, 05KhGB steels on the temperature of tempering*
Таблица 2. *Зависимость механических свойств, остаточных напряжений и плотности дислокаций сталей 08ХФА, 08ХМФА, 05ХГБ от температуры отпуска*

Steel grade	Heat treatment mode		σ_{UTS}, MPa	$\sigma_{0.2}$, MPa	δ, %	KCV-50, J/cm^2 (shear area fraction)	3rd type residual stresses, MPa	Dislocation density, $\rho\times10^{14}$, m^{-2}
	Quenching	Tempering						
08KhFA	930 °C	–	830	740	22.0	230 (100 %)	300	5.1
		200 °C	820	710	19.0	240 (100 %)	225	4.4
		300 °C	810	730	17.5	240 (100 %)	220	4.1
		400 °C	785	690	18.0	252 (100 %)	140	5.1
		500 °C	710	645	18.5	260 (100 %)	91	4.7
		600 °C	680	605	22.0	260 (100 %)	71	5.2
		700 °C	615	535	25.0	–	64	2.8
08KhMFA	930 °C	–	775	700	19.5	180 (80 %)	190	4.0
		200 °C	780	650	19.0	215 (100 %)	200	4.7
		300 °C	785	660	18.0	200 (100 %)	180	4.5
		400 °C	760	650	19.5	215 (100 %)	120	4.2
		500 °C	710	635	20.0	235 (100 %)	–	–
		600 °C	685	605	21.5	250 (100 %)	86	3.4
		700 °C	590	520	23.5	270 (100 %)	63	3.6
05KhGB	920 °C	–	605	490	29.0	290 (100 %)	570	5.4
		200 °C	–	–	–	–	–	–
		300 °C	590	500	29.0	315 (100 %)	460	4.9
		400 °C	560	470	27.0	330 (100 %)	215	4.7
		500 °C	530	430	28.0	314 (100 %)	90	4.5
		600 °C	510	420	27.0	325 (100 %)	45	4.0
		700 °C	–	–	–	–	–	–
Strength group K52			510–630	≥353	≥20	≥58,8	–	–

Table 3. *Dependence of corrosion properties of 08KhFA, 08KhMFA, 05KhGB steels on the temperature of tempering*
Таблица 3. *Зависимость коррозионных свойств сталей 08ХФА, 08ХМФА, 05ХГБ от температуры отпуска*

Steel grade	Heat treatment mode		Hydrogen cracking		Sulfide stress corrosion cracking		Carbon dioxide corrosion rate, mm/year
	Quenching	Tempering	CLR, %	CTR, %	% of σ_τ	K_{1SSC}, MPa/m$^{1/2}$	
08KhFA	930 °C	–	0	0	75	–	2.30
		200 °C				–	1.83
		300 °C				30.6	2.24
		400 °C				31.0	1.79
		500 °C				56.9	1.65
		600 °C				58.4	1.75
		700 °C				61.8	1.94
08KhMFA	930 °C	–	0	0	75	–	1.20
		200 °C					1.25
		300 °C					1.30
		400 °C					1.60
		500 °C					1.69
		600 °C					1.41
		700 °C					1.40
05KhGB	920 °C	–	0	0	70	–	2.07
		200 °C	–	–	–		–
		300 °C	0	0	70		2.07
		400 °C					1.93
		500 °C					1.93
		600 °C					1.40
		700 °C	–	–	–		–

Note. CLR is crack length ratio; CTR is crack thickness ratio; K_{1SSC} is critical stress intensity factor at the crack tip.
Примечание. CLR – коэффициент длины трещин; CTR – коэффициент толщины трещин;
K_{1SSC} – критический коэффициент интенсивности напряжений в вершине трещины.

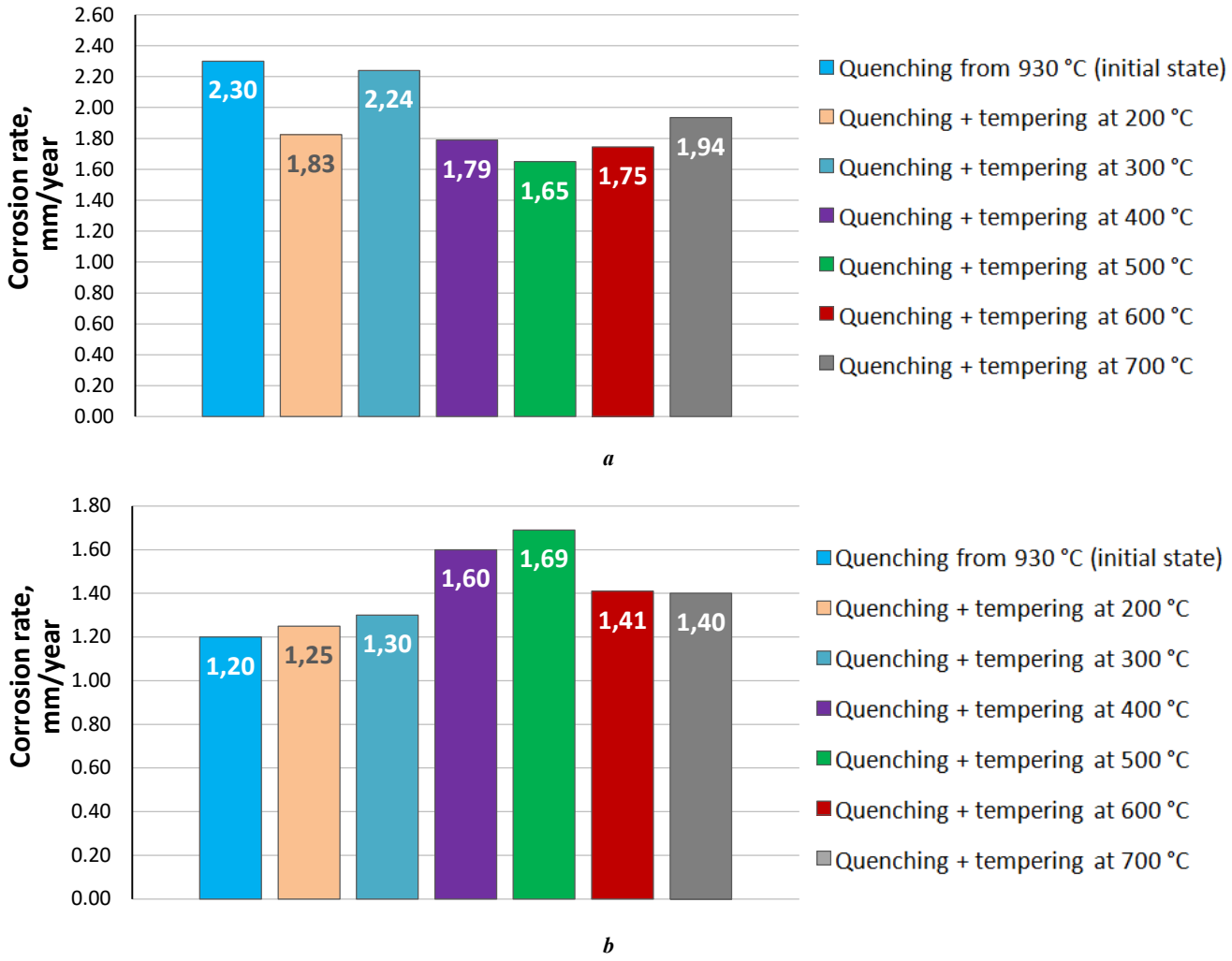

Fig. 6. *Carbon dioxide corrosion of 08KhFA and 08KhMFA steels.*
Dependence of corrosion rate on the temperature of tempering: ***a*** *– 08KhFA steel;* ***b*** *– 08KhMFA steel*
Рис. 6. *Углекислотная коррозия сталей 08ХФА и 08ХМФА.*
Зависимость скорости коррозии от температуры отпуска: ***а*** *– сталь 08ХФА;* ***b*** *– сталь 08ХМФА*

of a layer of corrosion products on the surface. Chromium and molybdenum are concentrated in corrosion products, and form amorphous $Cr(OH)_3$ and $Mo(OH)_3$ phases [21; 23], determining the protective properties of corrosion products. Only Cr and Mo contained in the solid solution participate in the formation of the protective properties of corrosion products. In a bound state in the form of carbides, they are inert and are excluded from the process. In the studied low-carbon steels, in the tempering temperature range of up to 600 °C, the formation of special carbides with the participation of Mo and Cr practically does not occur, and their concentration in the solid solution does not change. This, apparently, determines the absence of the effect of tempering on corrosion resistance. A slightly lower rate of carbon dioxide corrosion of 08KhMFA, steel compared to 08KhFA and 05KhGB steels (Table 3), is associated with the additional contribution of Mo to the protective properties of the corrosion products.

According to existing estimates, the studied steels have increased resistance to HC and SSCC under all heat treatment modes (Table 3). In SSCC tests, 08KhFA and 08KhMFA steels at a load of 0.75 σ_τ and 05KhGB steel at a load of 0.7 σ_τ withstood without destruction 720 h. However, the presence of high residual stresses after quenching and the anisotropy of the quenched structures determine the need for more stringent conditions for testing samples for SSCC resistance after quenching, and low-temperature tempering. It is proposed to conduct tests for SSCC at stresses of 0.8 or 0.85 of $\sigma_{0.2}$ determined in mechanical tensile tests for this group of samples.

The obtained data indicating that the resistance to carbon dioxide corrosion of steels, with a lath carbide-free bainite structure, does not change with increasing tempering temperature, allow choosing heat treatment modes more reasonably. In the production of pipes from low-carbon low-alloy steels with a bainite structure after water quenching, instead of traditional heat treatment (single or double quenching + high tempering), quenching from the austenitic region in water + medium tempering can be used, which provides a combination of higher strength properties with high corrosion resistance in aggressive oilfield environments. Medium tempering in steels with a lath carbide-free bainite structure, allows maintaining high strength properties,

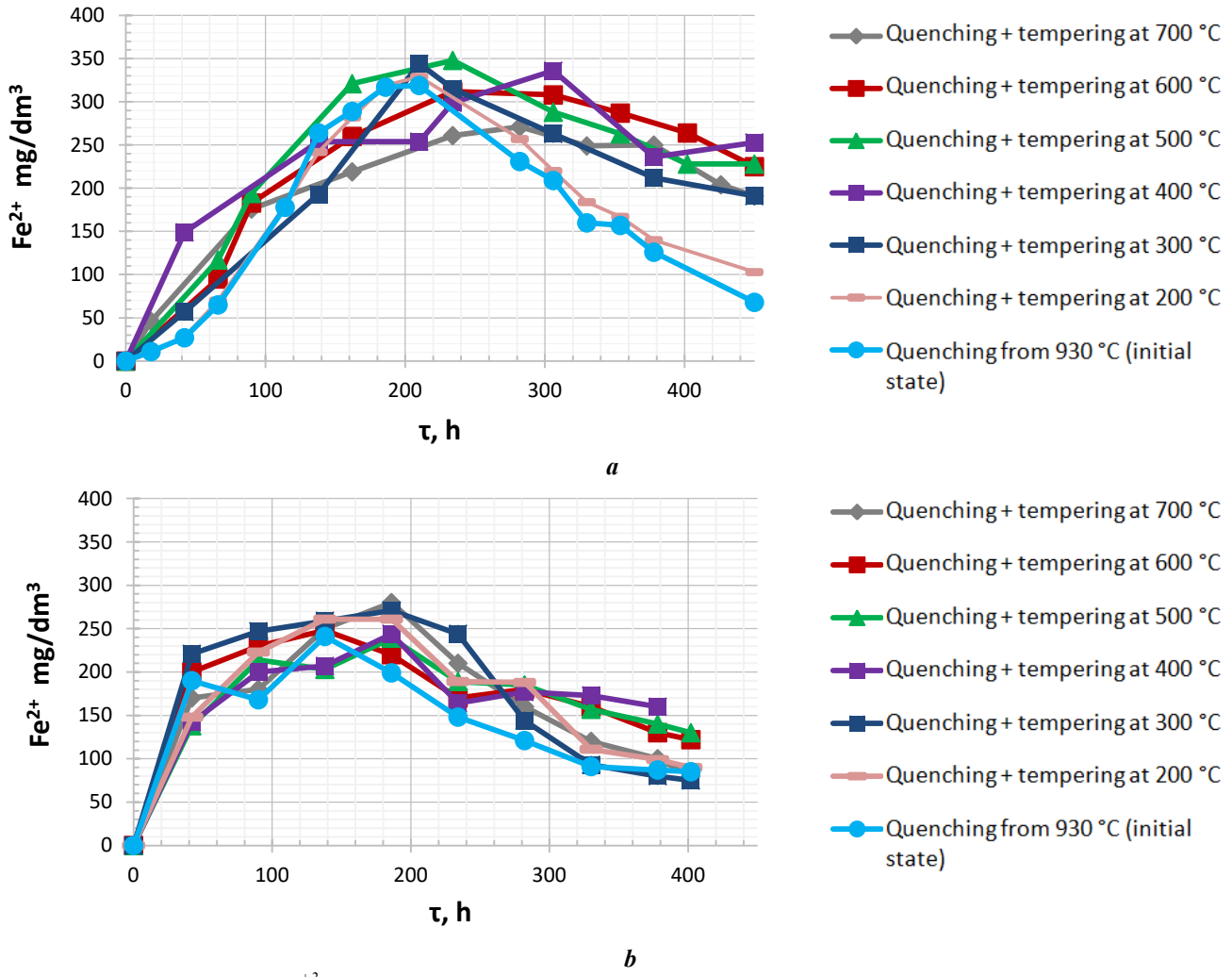

Fig. 7. *Dependence of the Fe^{+2} concentration in the model environment on the test time:* ***a*** *– 08KhFA steel;* ***b*** *– 08KhMFA steel*
Рис. 7. *Зависимость концентрации Fe^{+2} в модельной среде от времени испытаний:* ***а*** *– сталь 08ХФА;* ***b*** *– сталь 08ХМФА*

relieves the most dangerous residual stresses, and ensures the carbide phase formation. Tempering can be excluded or limited to low-temperature tempering for pipes operating in environments with a low H_2S content, or if the steel used withstands the more stringent SSCC tests proposed above. In the proposed heat treatment technology (without high tempering), microalloying of steel with V and Nb is advisable, when the precipitation of carbonitride particles of these elements occurs at the stage of formation of bainite structures.

CONCLUSIONS

1. The general structure type and mechanical properties of lath carbide-free bainite of low-carbon steels in the tempering temperature range up to 500 °C change insignificantly.

2. Tempering of lath carbide-free low-carbon bainite (08KhFA, 08KhMFA and 05KhGB steels), has little effect on its resistance to carbon dioxide corrosion.

3. Quenching and medium tempering in low-carbon low-alloy steels with bainitic hardenability, form a structural condition that ensures a combination of high mechanical properties, and high corrosion resistance in oilfield environments.

REFERENCES

1. Khromykh L.N., Litvin A.T., Nikitin A.V. Application of carbon dioxide in enhanced oil recovery. *Vestnik Evraziyskoy nauki*, 2018, vol. 10, no. 5, pp. 82–91. EDN: VRFXBN.
2. Efron L.I. *Metallovedenie v "bolshoy" metallurgii. Trubnye stali* [Metal science as part of "big" metallurgy. Pipe steel]. Moscow, Metallurgizdat Publ., 2012. 696 p.
3. Ioffe A.V. Assimilation of bainite structures in the production of pipe steels. *Perspektivnye materialy*. Tolyatti, TGU Publ., 2017. Vol. 6, pp. 153–196.
4. Yakovleva I.L., Tereshchenko N.A., Urtsev N.V. Observation of the martensitic-austenitic component in the structure of low-carbon low-alloy pipe steel. *Physics of Metals and Metallography*, 2020, vol. 121, no. 4, pp. 352–358. DOI: 10.1134/S0031918X20040171.
5. Rudskoy A.I. *Nauchnye osnovy upravleniya strukturoy i svoystvami staley v protsessakh termomekhanicheskoy obrabotki* [Scientific basis of controlling the structure and properties of steels in the heat treatment processes]. Moscow, RAN Publ., 2019. 276 p.
6. Maisuradze M.V., Ryzhkov M.A., Antakov E.V., Popov N.A., Proskuryakov P.A. Special features of trans-

formations of supercooled austenite in modern structural steels. *Metal Science and Heat Treatment*, 2020, vol. 62, no. 7-8, pp. 448–456. DOI: 10.1007/s11041-020-00583-4.
7. Mandal M., Poole W.J., Militzer M., Collons L. Temperature Dependence of Mechanical Properties for Advanced Line Pipe Steels With Bainitic Microstructures. *Metallurgical and Materials Transaction A*, 2023, vol. 54, pp. 3086–3100. DOI: 10.1007/s11661-023-07072-2.
8. Zajac S., Morris P., Komenda J. *Quantitative structure-property relationships for complex bainitic microstructures: final report*. Luxembourg, Office for Official Publications of the European Communities Publ., 2005. 161 p.
9. Ohmori Y., Ohtani H., Kunitake T. The Bainite in Low Carbon Low Alloy High Strength Steels. *Transactions of the Iron and Steel Institute of Japan*, 1971, vol. 11, no. 4, pp. 250–259. DOI: 10.2355/isijinternational1966.11.250.
10. Kaletin A.Y., Kaletina Y.V. The role of retained austenite in the structure of carbide-free bainite of construction steels. *Physics of Metals and Metallography*, 2018, vol. 119, no. 9, pp. 893–898. DOI: 10.1134/S0031918X18090053.
11. Kolbasnikov N.G., Zaitsev A.M., Adigamov R.R., Sakharov M.S., Matveev M.A. Role of Martensite-Austenite Component of Bainitic Structure in Formation of Properties of Pipe Steel. 3. Effect of Martensitic Transformation of Austenite in the MA-Component of Bainite on the Ductility of Steel. *Metal Science and Heat Treatment*, 2023, vol. 64, no. 9-10, pp. 547–553. DOI: 10.1007/s11041-023-00849-7.
12. Vyboishchik M.A., Gruzkov I.V., Chistopoltseva E.A., Tetyueva T.V. Formation of structure and properties of low-carbon bainite in steel 08KHFA. *Metal Science and Heat Treatment*, 2023, vol. 65, no. 7-8, pp. 400–409. DOI: 10.1007/s11041-023-00947-6.
13. Vyboyshchik M.A., Fedotova A.V., Chistopoltseva E.A., Kudashov D.V., Gruzkov I.V. Changes in structure and properties of low-carbon steel with structure of lath-type carbide-free bainite during tempering. *Deformatsiya i razrushenie materialov*, 2023, no. 8, pp. 31–39. DOI: 10.31044/1814-4632-2023-8-31-39.
14. Kolbasnikov N.G., Sakharov M.S., Kuzin S.A., Teteryatnikov V.S. Stability of untransformed austenite in M/A phase of bainitic structure of low-carbon steel. *Metal Science and Heat Treatment*, 2021, vol. 63, no. 1-2, pp. 63–69. DOI: 10.1007/s11041-021-00648-y.
15. Kolbasnikov N.G., Kuzin S.A., Teteryatnikov V.S., Adigamov R.R., Sakharov M.S., Matveev M.A. Role of bainitic structure martensitic-austenitic component in pipe steel property formation. 2. Austenite deformation and thermal stability. *Metal Science and Heat Treatment*, 2022, vol. 64, no. 3-4, pp. 137–145. DOI: 10.1007/s11041-022-00774-1.
16. Matrosov Yu.I. Mechanism of the influence of microadditions of niobium on microstructure and properties of thick-sheet low-alloy pipe steel. *Metal Science and Heat Treatment*, 2022, vol. 64, no. 1-2, pp. 87–94. DOI: 10.1007/s11041-022-00766-1.
17. Matrosov Yu.I. Comparison of the Effect of Microadditions of Niobium, Titanium and Vanadium on Formation of Microstructure of Low-Carbon Low-Alloy Steels. *Metal Science and Heat Treatment*, 2023, vol. 65, no. 3-4, pp. 152–158. DOI: 10.1007/s11041-023-00907-0.
18. Tetyueva T.V., Ioffe A.V., Denisova T.V., Trifonova E.A. special features of formation of structure in low-alloy steel 08KHMFBCHA upon quenching and tempering. *Metal Science and Heat Treatment*, 2013, vol. 54, no. 9-10, pp. 524–529. DOI: 10.1007/s11041-013-9542-7.
19. Zavalishchin A.N., Rumyantsev M.I., Kozhevnikova E.V. Effect of quenching and tempering on the structure and properties of hot-rolled pipe steels of strength categories K60 and K65. *Metal Science and Heat Treatment*, 2023, vol. 65, no. 1-2, pp. 12–17. DOI: 10.1007/s11041-023-00884-4.
20. Efron L.I., Stepanov P.P., Smetanin K.S., Vorkachev K.G., Kantor M.M., Bozhenov V.A. Questioning the effect of bainite morphology on the impact viscosity of low-carbon steels. *Steel in Translation*, 2021, vol. 51, no. 9, pp. 670–676. DOI: 10.3103/S0967091221090035.
21. Vyboyshchik M.A., Ioffe A.V. Scientific basis of development and the methodology of creation of steels for the production of oilfield casing and tubular goods with the increased strength and corrosion resistance. *Frontier materials and technologies*, 2019, no. 1, pp. 13–21. DOI: 10.18323/2073-5073-2019-1-13-20.
22. Li Y.Y., Wang Z.Z., Zhu G.Y., Zhang Q.H., Hou B.S., Lei Y., Wang X., Zhang G.A. Developing a water chemistry model in the CO_2-mixed salts – H_2O system to predict the corrosion of carbon steel in supercritical CO_2-containing formation water. *Corrosion Science*, 2021, vol. 192, article number 109806. DOI: 10.1016/j.corsci.2021.109806.
23. Keiichi K., Yoon-Shoi C., Srdjan N. Effect of Small Amount of Cr and Mo on Aqueous CO_2 Corrosions of Low-Alloyed Steel and Formation of Protective $FeCO_3$ in Near-Saturation Conditions. *Corrosion*, 2022, vol. 79, no. 1, pp. 97–110. DOI: https://doi.org/10.5006/4100.

СПИСОК ЛИТЕРАТУРЫ

1. Хромых Л.Н., Литвин А.Т., Никитин А.В. Применение углекислого газа в процессе повышения нефтеотдачи пластов // Вестник Евразийской науки. 2018. Т. 10. № 5. С. 82–91. EDN: VRFXBN.
2. Эфрон Л.И. Металловедение в «большой» металлургии. Трубные стали. М.: Металлургиздат, 2012. 696 с.
3. Иоффе А.В. Освоение бейнитных структур в производстве трубных сталей // Перспективные материалы. Т. 6. Тольятти: ТГУ, 2017. С. 153–196.
4. Яковлева И.Л., Терещенко Н.А., Урцев Н.В. Наблюдение мартенситно-аустенитной составляющей в структуре низкоуглеродистой низколегированной трубной стали // Физика металлов и металловедение. 2020. Т. 121. № 4. С. 396–402. DOI: 10.31857/S0015323020040178.

5. Рудской А.И. Научные основы управления структурой и свойствами сталей в процессах термомеханической обработки. М.: РАН, 2019. 276 с.
6. Майсурадзе М.В., Рыжков М.А., Антаков Е.В., Попов Н.А., Проскуряков П.А. Особенности превращений переохлажденного аустенита в современных конструкционных сталях // Металловедение и термическая обработка металлов. 2020. № 7. С. 29–38. EDN: AEAGTO.
7. Mandal M., Poole W.J., Militzer M., Collons L. Temperature Dependence of Mechanical Properties for Advanced Line Pipe Steels With Bainitic Microstructures // Metallurgical and Materials Transaction A. 2023. Vol. 54. P. 3086–3100. DOI: 10.1007/s11661-023-07072-2.
8. Zajac S., Morris P., Komenda J. Quantitative structure-property relationships for complex bainitic microstructures: final report. Luxembourg: Office for Official Publications of the European Communities, 2005. 161 p.
9. Ohmori Y., Ohtani H., Kunitake T. The Bainite in Low Carbon Low Alloy High Strength Steels // Transactions of the Iron and Steel Institute of Japan. 1971. Vol. 11. № 4. P. 250–259. DOI: 10.2355/isijinternational1966.11.250.
10. Калетин А.Ю., Калетина Ю.В. Роль остаточного аустенита в структуре бескарбидного бейнита конструкционных сталей // Физика металлов и металловедение. 2018. Т. 119. № 9. С. 946–952. DOI: 10.1134/S001532301809005X.
11. Колбасников Н.Г., Зайцев А.М., Адигамов Р.Р., Сахаров М.С., Матвеев М.А. О роли мартенситно-аустенитной составляющей бейнитной структуры в формировании свойств трубной стали. 3. Влияние мартенситного превращения аустенита в МА-составляющей бейнита на пластичность стали // Металловедение и термическая обработка металлов. 2022. № 10. С. 12–19. DOI: 10.30906/mitom.2022.10.12-19.
12. Выбойщик М.А., Грузков И.В., Чистопольцева Е.А., Тетюева Т.В. Формирование структуры и свойств низкоуглеродистого бейнита в стали 08ХФА // Металловедение и термическая обработка металлов. 2023. № 7. С. 8–16. DOI: 10.30906/mitom.2023.7.8-16.
13. Выбойщик М.А., Федотова А.В., Чистопольцева Е.А., Кудашов Д.В., Грузков И.В. Изменение структуры и свойств низкоуглеродистой стали со структурой реечного бескарбидного бейнита в процессе отпуска // Деформация и разрушение материалов. 2023. № 8. С. 31–39. DOI: 10.31044/1814-4632-2023-8-31-39.
14. Колбасников Н.Г., Сахаров М.С., Кузин С.А., Тетерятников В.С. О стабильности непревращенного аустенита в М/А – фазе бейнитной структуры низкоуглеродистой стали // Металловедение и термическая обработка металлов. 2021. № 2. С. 3–10. EDN: BPZXXG.
15. Колбасников Н.Г., Кузин С.А., Тетерятников В.С., Адигамов Р.Р., Сахаров М.С., Матвеев М.А. О роли мартенситно-аустенитной составляющей бейнитной структуры в формировании свойств трубной стали. 2. Деформационная и термическая стабильность аустенита // Металловедение и термическая обработка металлов. 2022. № 3. С. 3–12. DOI: 10.30906/mitom.2022.3.3-12.
16. Матросов Ю.И. Механизм влияния микродобавок ниобия на микроструктуру и свойства толстолистовых низколегированных трубных сталей // Металловедение и термическая обработка металлов. 2022. № 2. С. 18–26. DOI: 10.30906/mitom.2022.2.18-26.
17. Матросов Ю.И. Сопоставление влияния микродобавок Nb, Ti, V на процессы формирования микроструктуры низкоуглеродистой низколегированной стали. // Металловедение и термическая обработка металлов. 2023. № 3. С. 25–31. DOI: 10.30906/mitom.2023.3.25-31.
18. Тетюева Т.В., Иоффе А.В., Денисова Т.В., Трифонова Е.А. Особенности формирования структуры в низкоуглеродистой стали 08ХМФБЧА при закалке и отпуске // Металловедение и термическая обработка металлов. 2012. № 10. С. 34–38. EDN: PHHLAT.
19. Завалищин А.Н., Румянцев М.И., Кожевникова Е.В. Влияние закалки и отпуска на структуру и свойства горячекатаного проката из сталей трубного сортамента категорий прочности К60 и К65 // Металловедение и термическая обработка металлов. 2023. № 1. С. 13–18. DOI: 10.30906/mitom.2023.1.13-18.
20. Эфрон Л.И., Степанов П.П., Воркачев К.Г., Кантор М.М., Боженов В.А., Сметанин К.С. К вопросу о влиянии морфологии бейнита на ударную вязкость низкоуглеродистых сталей // Сталь. 2021. № 9. С. 45–50. EDN: XYMRAF.
21. Выбойщик М.А., Иоффе А.В. Научные основы разработки и методология создания сталей для производства нефтепромысловых труб, повышенной прочности и коррозионной стойкости // Вектор науки Тольяттинского государственного университета. 2019. № 1. С. 13–21. DOI: 10.18323/2073-5073-2019-1-13-20.
22. Li Y.Y., Wang Z.Z., Zhu G.Y., Zhang Q.H., Hou B.S., Lei Y., Wang X., Zhang G.A. Developing a water chemistry model in the CO_2-mixed salts – H_2O system to predict the corrosion of carbon steel in supercritical CO_2-containing formation water // Corrosion Science. 2021. Vol. 192. Article number 109806. DOI: 10.1016/j.corsci.2021.109806.
23. Keiichi K., Yoon-Shoi C., Srdjan N. Effect of Small Amount of Cr and Mo on Aqueous CO_2 Corrosions of Low-Alloyed Steel and Formation of Protective $FeCO_3$ in Near-Saturation Conditions // Corrosion. 2022. Vol. 79. № 1. P. 97–110. DOI: https://doi.org/10.5006/4100.

Коррозионно-механическое разрушение бейнитных структур в нефтепромысловых средах

Выбойщик Михаил Александрович[1,3], доктор физико-математических наук, профессор, профессор кафедры «Сварка, обработка материалов давлением и родственные процессы»
Грузков Игорь Викторович*[1,2,4], аспирант, заведующий лабораторией оптической и электронной микроскопии
[1]*Тольяттинский государственный университет, Тольятти (Россия)*
[2]*ООО «ИТ-Сервис», Самара (Россия)*

***E-mail:** gruzkov@its-samara.com, gigabon7@mail.ru
[3]ORCID: https://orcid.org/0000-0003-2797-5396
[4]ORCID: https://orcid.org/0009-0007-9580-9935

Поступила в редакцию 12.12.2023 *Принята к публикации 15.08.2024*

Аннотация: Основным направлением в решении проблемы повышения надежности промыслового оборудования является создание новых сталей с более высоким сопротивлением коррозионно-механическому разрушению. В настоящее время для изготовления нефтегазопроводных систем используются низкоуглеродистые низколегированные стали, в которых при закалке в воду образуется реечный бескарбидный бейнит. Такая структура дает сочетание высокой прочности и сопротивления хрупкому разрушению. Однако вопросы повышения коррозионной стойкости остаются нерешенными. Цель работы – установить структурное состояние низкоуглеродистых низколегированных трубных сталей, обеспечивающее сочетание высоких механических свойств с повышенной коррозионной стойкостью в нефтепромысловых средах. Исследования проводились на сталях последнего поколения 08ХФА, 08ХФМА и 05ХГБ, наиболее распространенных при изготовлении нефтегазопроводных труб. Образцы для исследования вырезались из труб и закаливались из аустенитной области в воду, что формировало структуру реечного бескарбидного бейнита. Закаленные образцы подвергались отпуску при температурах 200, 300, 400, 500, 600 и 700 °С. Для установления связи между морфологией бейнитных структур и их свойствами образцы после закалки и отпуска с каждой температуры подвергались металлографическому анализу, рентгеноструктурному анализу, механическим испытаниям, испытаниям на стойкость к коррозии. В работе показаны последовательность трансформации структуры, температурные интервалы фазовых и структурных превращений, изменения механических свойств и коррозионной стойкости, происходящие при отпуске реечного бескарбидного низкоуглеродистого бейнита. Показано, что отпуск реечного бескарбидного бейнита (стали 08ХФА, 08ХМФА и 05ХГБ) не влияет на скорость углекислотной коррозии. Установлено, что средний отпуск формирует структурное состояние бескарбидного низкоуглеродистого реечного бейнита, обеспечивающее сочетание высоких механических свойств и высокой коррозионной стойкости в нефтепромысловых средах. Для каждой из исследуемых сталей приводятся рекомендуемые режимы термообработки.

Ключевые слова: коррозионно-механическое разрушение; разрушение бейнитных структур; нефтепромысловая среда; трубные стали; структурное состояние.

Для цитирования: Выбойщик М.А., Грузков И.В. Коррозионно-механическое разрушение бейнитных структур в нефтепромысловых средах // Frontier Materials & Technologies. 2024. № 3. С. 17–29. DOI: 10.18323/2782-4039-2024-3-69-2.